An Investigation of the Neuronal Dynamics Under Noisy Rate Functions

Renas Rajab Asaad

Submitted to the
Institute of Graduate Studies and Research
in partial fulfillment of the requirements for the Degree of

Master of Science
in
Computer Engineering

Eastern Mediterranean University
June 2014
Gazimağusa, North Cyprus

Approval of the Institute of Graduate Studies and Research

Prof. Dr. Elvan Yılmaz
Director

I certify that this thesis satisfies the requirements as a thesis for the degree of Master of Science in Computer Engineering.

Prof. Dr. Işık Aybay
Chair, Department of Computer Engineering

We certify that we have read this thesis and that in our opinion it is fully adequate in scope and quality as a thesis for the degree of Master of Science in Computer Engineering.

Prof. Dr. Marifi Güler
Supervisor

Examining Committee

1. Prof. Dr. Erden Başar

2. Prof. Dr. Marifi Güler

3. Asst. Prof. Dr. Yıltan Bitirim

ABSTRACT

In latest years, it has been argued theoretically and shown both by experiments and by numerical simulations that noise of ion channel in neurons can have profound effect on the dynamical behavior of neuron when the size of membrane area is limited. Different models that extend the Hodgkin-Huxley equations into stochastic differential equations to capture the effects of ion channel noise analytically have been put forward: the Fox-Lu model, the Linaro-Storace-Giugliano model, and the Güler model. Moreover, very recently it has been argued by Güler that the rate functions for the opening and closing of gates are under the influence of noise in small size neurons.

In this thesis, the neuronal dynamics with subject to noise in the rate functions will be investigated thoroughly. The investigation will employ the exact Markov simulations and the above analytical models. Results from these models will be presented comparatively. The study aims at presenting a more detailed account on the phenomenon already outlined by Güler recently.

Keywords: Ion Channels, Channel Noise, Colored Noise, The Channel Crossing, Small-sized Dice, Stochastic Hodgkin-Huxley.

ÖZ

Son yıllarda, nöronlardaki ion kanal gürültüsünün küçük boyutlu nöron dinamiği üzerinde hayati etki yapabildiği deneysel olarak ve sayısal benzetim yöntemleri kullanarak kanıtlanmıştır. Sözkonusu etkinin analitik olarak ifade edilmesine yönelik olarak farklı gruplar Hodgkin-Huxley denklemlerini stokastik diferansiyel denklem haline dönüştürmüştür: Fox-Lu (1994); Linaro, Storace ve Giugliano (2011); Güler (2013a). Daha yakın zamanda, Güler (2013b) tarafından geçit kapanım-açılım oran fonksiyonlarının gürültülü olabildiği öne sürülmüştür.

Bu tezde, yukarıdaki stokastik Hodgkin-Huxley modelleri gürültülü oran fonksiyonları altında çalışılmıştır. Güler (2013a) modelinin diğer modellere göre mikroskopik benzeşim sonuçlarıyla çok daha uyumlu olduğu gözlenmiştir.

Anahtar Kelimeler: İyon kanalı, Kanal gürültüsü, Renkli gürültü, Kanal geçiti, Küçük boyutlu zar, Stokastik Hodgkin-Huxley.

DEDICATION

To my Lovely Family

To my Brothers and Sisters

R.R.R

ACKNOWLEDGMENT

I sincerely acknowledge to my father and mother for them supports and help that gave to me, my parents who I owe my all life and also my graduation and all successes to them.

I would like to acknowledge with gratitude Prof. Dr. Marifi Güler without his guidance, knowledge, and effort this research will be imposable.

TABLE OF CONTENTS

LIST OF TABLES

LIST OF FIGURES

Chapter 1

INTRODUCTION

The Effect of noise to the neurons produces an unusual pattern on the neuronal dynamics. The noise is in two types; internal or external (Faisal A. S., 2008). External noise is exactly the opposite of internal. External noise is produced from the synaptic signal transmission. The prime source of internal noise in a neuronal membrane spot is from the limited number of voltage-gated ion channels. Usually these channels have two stats; closed or open. When it is open, the channel's fluctuations number is apparently going randomly (Sakmann, 1995). If fluctuations are included in the membrane conduct, then fluctuation will be included in the voltage of transmembrane as well. When the number of ion channels is large means that the membrane size is huge, the voltage dynamics will represent as in the original Hodgkin and Huxley (Hodgkin, 1952) equation. However, when the patch of membrane is small, the conductance fluctuations affect the voltage activity of the cell. These effects are probably important and cannot be ignored. The single open channel stochasticity effect in a direct manner the spike behaviour which is suggested by experiment investigation ((Sigworth, 1980); (Lynch, 1989); (Johansson, 1994)), and spontaneous fire will be the result of that noise in the ion channels ((Koch, 1999);(White, 1998)). Patch-clamp experiments *in vitro* have demonstrated that the noise of channel in the dendrites also in the soma resulting voltage fluctuations that are large enough to affect asynchronies in the timing, initiation, and

propagation of action potentials ((Diba, 2004); (Jacobson, 2005); (Dorval, 2005); (Kole, 2006)).

The phenomenon called stochastic resonance has been observed to occur in a system of voltage-dependent ion channels formed by the peptide alamethicin ((Bezrukov, 1995)).

Spontaneous spiking is a phenomenon caused by the internal noise from the ion channels. Proof through theoretical investigations and numerical simulations of channel dynamics (in the form of repetitive spiking or bursting), or in otherwise quiet membrane patches ((DeFelice, 1992); (Strassberg, 1993); (Chow, 1996); (Rowat, 2004); (Güler, 2007) ;(Güler, 2008);(Güler, 2011); (Güler, 2013a)); furthermore, these investigations also have revealed the occurrence of stochastic resonance and the coherence of the generated spike trains ((Jung, 2001); (Schmid, 2001); (Özer, 2006)). In addition, the channel fluctuations might reach the critical value near from the action potential threshold even if the numbers of existed ion channels are large. ((Schneidman, 1998); (Rubinstein, 1995)); The timing accuracy of an action potential is measured by a small number of opening ion channel at that threshold. Furthermore, ion channel noise controls the spike propagation in axons ((Faisal A. A., 2007); (Ochab-Marcinek, 2009)), The DSM model accommodates some functional forms called the renormalization terms, in addition to some white noise terms of vanishing, in the equations of activity. The DSM model has been investigated in detail numerically for its dynamics for time-independent input currents (Güler 2008); it was found that the renormalization corrections augment the behavioural transitions from quiescence to spiking and from tonic firing to bursting. It was also found that the presence of renormalization corrections can lead to faster temporal synchronization of the respective discharges of electrically coupled two

neuronal units (Jibril and Güler 2009). More recently, a stochastic Hodgkin – Huxley model, having colored noise terms in the conductances was proposed (Güler, 2013a), where the colored terms capture those effects due to the gate multiplicity.

1.1 Scope and organization

In this thesis, the neuronal dynamics with subject to noise in the rate functions will be thoroughly investigated. The investigation will employ the exact Markov simulations and the above analytical models. The results from these models will be presented comparatively. The study aims at presenting a more detailed account on the phenomenon already outlined by Güler.

This thesis is divided into six chapters. Chapter 1 describes introduction about thesis. Chapter 2 describes Morphological and structural of neurons. Chapter 3 describes modeling the excitability of neurons. Chapter 4 describes the dynamics membrane. Chapter 5 describes the numerical experiments and chapter six is the conclusion about thesis.

Chapter 2

MORPHOLOGY AND STRUCTURE OF NEURONS

2.1 Introduction

Neurons are the main types of cells in human brain; they're most significant concept in human brain that are exclusive in generating electrical signals reasoned to chemical and other inputs. Furthermore, the approximate number of neurons in human brain is 100 billion, each one with a unique group of thousands inputs. They can transfer signals to other neurons via synapses. There are three parts of normal neurons: somas, dendrites, axons. The electrical signals can be transferred via dendrites to other neurons that are around synapses and sent to the body defined as soma, and the axons for transferring the output of neural to other cells. The estimated connections of axons with synapses are 180 per μm. The structure of dendritic increases the superficies area of the cell to help neurons for receiving inputs from large number of neurons by synapses. Commonly, the dendrites receive two signals from other neural. The soma of optimal skin of neurons moves in diagonal between 10 to 25 μm. The neuron contains two parts: Spike and membrane potential, shows in figure (1).

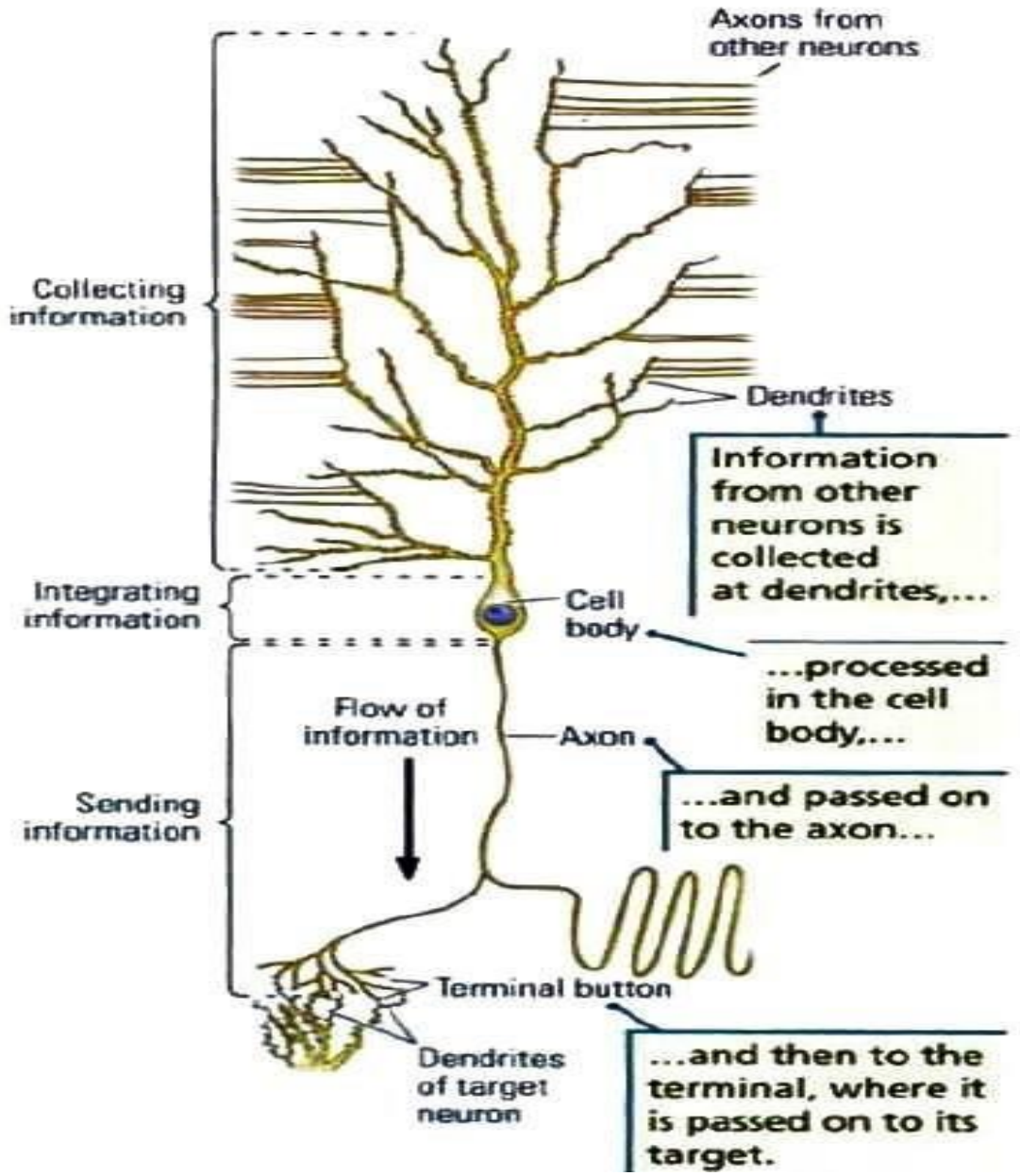

Figure 1: Two Interconnected Cortical Pyramidal Neurons (Izhikevich, 2007)

Figure 1 shows in details the information flow and neuron structure. Crossing huge fractions of the brain by axon of a single neuron, dendrite collects the information of other neuron, then processes in the body of cell and passed on to the axon. Soma, or the body of the cell of neurons, ranges between 10 to 50 μm (Dayan Abbot, 2002).

2.1.1 Spike

The communication between neurons is simple. Each neuron received a spike from 10,000 neurons via synapse. The transmembrane current, that changes the potential of membrane, caused because of transferring electrical signals. The post synapse potentials (PSPS) are current signals received from synapse. Spike, or action potential, is generated because of voltage sensitive channel in a neuron (Izhikevich, 2007).

2.1.2 Membrane proteins

Proteins in neuron cell membrane are classified into three groups to transport substances through other. To understand the functions of neurons one should be familiar with some information about these proteins. These three groups: channels, gates, pumps, help to convey the materials through the membrane. In this research, only the first two groups will be studied.

2.1.2.1 Channels

Some membranes proteins are designed to create channels or holes, to allow some substance pass through it. Various kinds of proteins with various size of holes pass in or out of the cell. Each channel can allow one of the potassium and sodium to pass through it, different range of voltage can control to pass one of them through a channel. Protein molecules work as channel, like potassium $(K+)$, sodium $(Na+)$, chloride $(CL-)$, and calcium $(Ca++)$.

2.1.2.2 Gates

One of the significant features of protein molecules is the ability of changing its form called gates. The gates change its form when different chemicals are bound to them, it allows some specific chemicals to cross through it, and in these cases, it serves as a door lock. It will be active when the key matches with the embedded proteins by the

size and its form. Moreover, there are some different types of gates responsible for different motions such as temperature change or electrical charge to allow assured chemical to across through it.

2.2 Neuron Electrical Activity and Membrane Potential

Membrane potential's simple definition is the electrical potential or difference of potential between the interior and extracellular fluid of the neuron. In some situations like resting state, the electrical potential of the cell membrane inside the neuron is about -70mV relative to the a rounding path. Nevertheless, this action potential is traditionally supposed to be zero mV for more convenience, and in this situation the cell state is said to be polarized. This potential is in a balance point at which the ions that flow outside matches with those that flow inside. The difference made by membrane potential is continued by ion pumps in maintaining concentration on gradient placed in the cell membrane. For example, concentration of sodium $(Na+)$ is much more outside of a neuron than inside, and the $(K+)$concentrated inside of a neuron more than outside of it. As a result, ions flow into and out of a cell because of concentration gradients and voltage during the state transition of cell.

Current, the flowing of ions form affected to state transition of neuron to flowing out of the cell, is caused by voltage and concentration gradients. Current is produced by positive charge. Through open channels this current flows out of the neuron making membrane potential more negatively increased. This phenomenon is called hyper polarization. The depolarization process occurs when the current streaming inside the cell changes to be negative of the membrane potential or even to be positive, when the neuron depolarization is large enough to increase the membrane potential more than the threshold level, an operation with positive feedback will start and makes the

neuron to generate an action potential and this action is nearly 100 mV fluctuation in the voltage potential passing through the cell membrane that is just about one 1ms. Once an action potential occurs and is used to equalize it between inside and outside the neuron, it's impossible to start with another spike directly after the former one is called absolute refractory period. The difference between the action potential and subthreshold fluctuation could be summarized by propagation over long distance. In action, potential almost reaches 1 millimeter and the propagation of the signal without attenuation (Abbot, 2002).

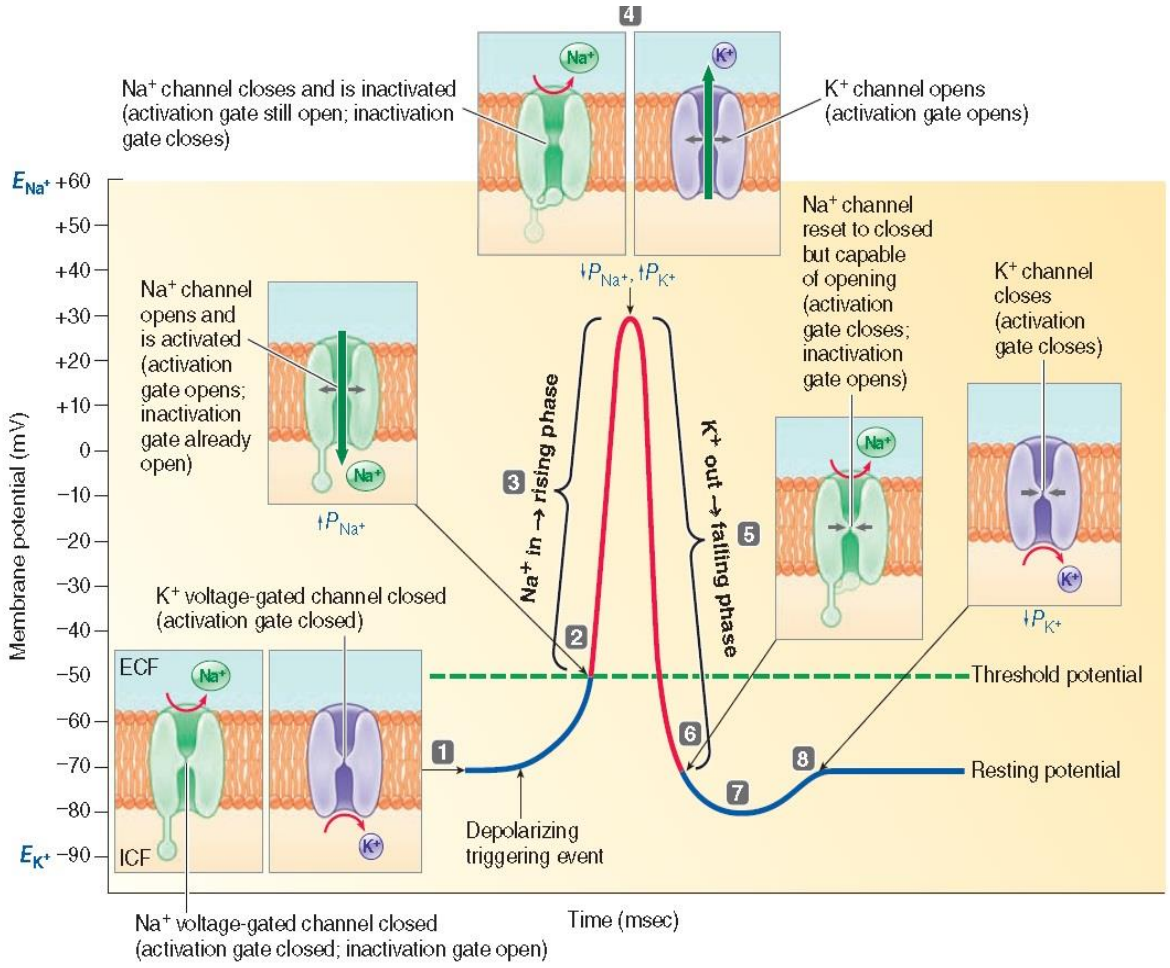

1 Resting potential: all voltage-gated channels closed.

2 At threshold, Na^+ activation gate opens and P_{Na^+} rises.

3 Na^+ enters cell, causing explosive depolarization to +30 mV, which generates rising phase of action potential.

4 At peak of action potential, Na^+ inactivation gate closes and P_{Na^+} falls, ending net movement of Na^+ into cell. At the same time, K^+ activation gate opens and P_{K^+} rises.

5 K^+ leaves cell, causing its repolarization to resting potential, which generates falling phase of action potential.

6 On return to resting potential, Na^+ activation gate closes and inactivation gate opens, resetting channel to respond to another depolarizing triggering event.

7 Further outward movement of K^+ through still-open K^+ channel briefly hyperpolarizes membrane, which generates after hyperpolarization.

8 K^+ activation gate closes, and membrane returns to resting potential.

Figure 2: Action potential phases (Whishaw, 2012)

Figure 2 discusses the dynamic voltages during an action potential while the synchronization by conforming ion channels actions. As shown in figure 2 the resting potential in real value -70mV.

Chapter 3

MODELLING THE EXCITABILITY OF NEURON

3.1 Introduction

Over the last 60 years ago, many models of neurons were developed by scientists for various purposes. Furthermore, these models range from structurally biophysical models, for example, one of the most significant models is Hodgkin-Huxley (HH), and the one that this thesis focuses on the neuronal dynamics under noise rate functions (set by Güler(2013b)). In various studies, different models may be needed depending on models' biological features, their complexity and the implementation cost. Nevertheless, a technique of neural excitability modeling is linked from the monument work of HH model (1952).

3.2 The Hodgkin-Huxley Model

Based on a lot of investigations, experiment conducted on giant squid axon by using voltage clamp and space clamp, Hodgkin-Huxley (1952) model shows the current crossing through the squid axon membrane had two main ionic elements I_K (potassium channel current) and I_{Na} (sodium channel current). The membrane potential V_m is hugely controlled by these currents.

They consequently developed a mathematical model of their observation to make a model which is still most significant one based on which many realistic neural models have been developed (Hodgkin-Huxley 1952).

In the Hodgkin-Huxley model, the part of nerve membrane had electrical characteristics that could be represented by an equivalent circuit in which current flow across the membrane has two major parts, the first one concerned with charging capacitance of membrane, and the other one concerned with movement of special type of ions across the membrane. In addition, the ionic is classified to three elements, a potassium current I_K, a sodium current I_{Na}, a small leakage I_L that is primarily conveyed by chloride ions.

The differential equation similar to the electrical circuit is like follows

$$C_m \frac{dv_m}{dt} + I_{ion} = I_{ext} \quad (1)$$

$C_m$is membrane capacitance.

$V_m$is membrane potential.

$I_{ext}$is an externally current.

$I_{ion}$is the ionic current.

The I_{ion} is the current inflow into the membrane and can be considered from the following equations:

$$\mathrm{I_{ion}} = \sum_{\mathrm{i}} \mathrm{I_i} \quad (2)$$

$$\mathrm{I_i} = \mathrm{g_i}(\mathrm{V_m} - \mathrm{E_i}) \quad (3)$$

I_i here denotes every ionic current component having related to conductance g_i and reversal potential E_i.

There are three I_i of the giant squid axon, potassium current I_K, sodium current I_{Na}, and leakage I_L, that will give us these equations:

$$I_{ion} = I_{Na} + I_K + I_L \quad (4)$$

$$I_{Na} = g_{Na}(V_m - E_{Na}) \quad (5)$$

$$I_K = g_K(V_m - E_K) \quad (6)$$

$$I_L = g_L(V_m - E_L) \quad (7)$$

The conductance of microscopic $g_i(g_{Na}, g_K, g_L)$ grows from the merge influence of amount number of membrane microscopic ion channel. Ion's current can be considered as containing a few numbers of physical gates, that regulate the ions flow across the channel. While the channel opens all the gates in the permissive state, ions can flow through the channel.

3.3 The ionic conductance

The Hodgkin-Huxley model supposes the priori experience of the Markov kinetic process based on each gate. If an n-gate is open at time *t* it will be open till time $t + \Delta t$ with probability given by $\exp(-\beta_n \Delta t)$, and if an n-gate is closed at time t it will stay closed at time $t + \Delta t$ with given probability by $\exp(-\alpha_n \Delta t)$. And the $\alpha_n and \beta_n$ are opening and closing gates. There are three m-gates and one h-gate for sodium channel and four n-gates for potassium channel (Güler, 2013a). Consequently, the detection of the experimental of a voltage current influx within the membrane, correlating with the movement of some charged particles called particles gating (Schneider & Chandler,1973; Armstrong &Bezanilla,1973; Keynes & Rojas,1974).There is a suspicion that the conducting state of a channel depends on the binding of a gating charge (or gating particles) to the external channel gate face

of the membrane. This gating charge can grow up from charged remains on the protein, for instance, in the S4 fourth trans-membrane segment, or from charged ligands binding to deep locations within the protein. Gating include sensitive temperature conformational changes of channel proteins. Molecular modeling and structure function learns indicate a sliding-helix mechanism for electromechanical conjunction in which the exterior movement of gating charges in the fourth trans-membrane segments pulls the S4-S5 connector, curvatures the S6 segment, and opens the pore. (For an extensive overview of the subject, see Hille, 2001, and Catterall, 2010.)

The Hodgkin-Huxley models combine some noise terms into the deterministic Hodgkin-Huxley equations as follows:

$$\dot{n} = \alpha_n(n-1) - \beta_n n + \eta_n \quad (8)$$

$$\dot{m} = \alpha_m(m-1) - \beta_m m + \eta_m \quad (9)$$

$$\dot{h} = \alpha_h(h-1) - \beta_h h + \eta_h \quad (10)$$

Here $\eta_n, \eta_m, and \eta_h$ are the mean zero noise terms; they vanish in of infinite limit of the membrane size. Here $(\alpha_n, \alpha_m, \alpha_h)$ and $(\beta_n, \beta_m, \beta_h)$ are rate constants.

Experiment on voltage clamp of the membrane potential will start resting at state $(V_m = 0)$ and immediately stepped to a new voltage clamp $(V_m = V_c)$. The answer by exponential of the form is to the equation (9) as shown below:

$$\chi(t) = \chi_\infty(V_c) - (\chi_\infty(V_c) - \chi_\infty(0))\exp(-\frac{t}{\tau_\chi}) \quad (11)$$

$$\chi_\infty(0) = \frac{\alpha_\chi(0)}{\alpha_\chi(0)} + \beta_\chi(0) \quad (12)$$

$$\chi_\infty(V_c) = \frac{\alpha_\chi(V_c)}{\alpha_\chi(V_c)} + \beta_\chi(V_c) \quad (13)$$

$$\tau_\chi(V_c) = [\alpha_\chi(V_c) + \beta_\chi(V_c)]^{-1} \quad (14)$$

Here χ defined as a time depending variable of gate $(n, m, \text{and h})$, the value of voltage of gating variable has been determined at resting state, means the $\chi_\infty(0) = 0$ and $\chi_\infty(V_c) = 0$ the clamp voltage V_c to make the formula simple. τ_χ denotes the constant time course for approaching the steady state value of $\chi_\infty(V_c)$ when the voltage is clamped to (V_c). Hodgkin and Huxley considered stables α_i, β_i as functions of V in the following form:

$$\alpha_i = \chi_\infty(V)/\tau_n(V) \quad (15)$$

$$\beta_i = 1 - \chi_\infty(V)/\tau_n(V) \quad (16)$$

i denoted for $(n, m, \text{and h})$ion channel gate variables as mentioned before.

These formulas state for the constants rate of α_i, β_i that are concluded experimentally:

$$\alpha_n(V) = \frac{0.01(10-V)}{\exp\left(\frac{(10-V}{10}\right)-1} \quad (17)$$

$$\beta_n(V) = 0.125 \exp(-\frac{V}{80}) \quad (18)$$

$$\alpha_m(V) = \frac{0.1(25-V)}{\exp\left(\frac{(10-V}{10}\right)-1} \quad (19)$$

$$\beta_m(V) = 4 \exp\left(-\frac{V}{18}\right) \quad (20)$$

$$\alpha_h(V) = 0.07 \exp(-\frac{V}{20}) \quad (21)$$

$$\beta_h(V) = \frac{1}{\exp\left(\frac{(30-V}{10}\right)+1} \quad (22)$$

3.4 Stochastic Models

Neurons exhibit electrical action, and it's in nature known to be stochastic (Faisal, 2008). The main source of stochasticity from the synapses is the external noise. The interior noise, which participates to the gating probabilistic nature of the ion channel, can have important effects on the neuron's dynamic performance as it is displayed in the experimental studies (Kole, 2006; Jacobson et al., 2005; Sakmann and Neher, 1995), and by theoretical researches numerical simulations (Chowand White, 1996; Fox and Lu, 1994; Schmid et al., 2001; Schneidman et al., 1998). Neuronal dynamics under the effect of channel fluctuation is usually modeled with stochastic differential equations acquired by using some vanishing white-noise conditions in to the fundamental deterministic equations (Fox and Lu, 1994). The dissipative stochastic mechanics (DSM neuron) based on the neuron model raised by Güler (2007, 2008), is a special case of it. The DSM model has some forms of functionality named the re-normalization terms, as well as some vanishing white-noise conditions in the activity equations. The DSM model has been studied in numerical details for its time independent input current's dynamics (Güler, 2008); it was established that the corrections of re-normalization increase the changes in behavior from quiescence to spiking and from tonic firing to bursting. It was further stated, that the existence of re-normalization corrections can result in faster temporal synchronization of the electric coupled consecutive, and it charges of two neuronal units (Jibril and Güler, 2009).

3.5 The DSM Neuron Model

The DSM (Dissipative Stochastic Mechanics) based on neuron special formulation stems from a viewpoint that ion channel conformational changes are exposed to two distinct types of noise. These two types of noise were coined as topological noise and the intrinsic noise. The intrinsic noise gets up from gating particles voltage, and is stochastic between (outer, inner) of the membrane. Accordingly, gates close and open in a probabilistic style, it's the average and by this average the opening gates in the membrane is defined. The topological noise, on the other hand, are stems from the existence of a various number of gates in the channels, and it contributes to the changes in the topology of open gates, rather than the changes in the number of open gates.

Indecencies, throughout the dynamics, avoid following a specific order in occupying the available closed gates like gating particles, thus, in resting the open gates at two distinct times the membrane may have the same number of open gates but two various conductance values. The topological noise is attributed to the uncertainty in the open channels numbers that takes place even if the number of open gates is precisely known in defining the voltage dynamics.

DSM neuron formula was developed based on Hindmarsh-Rose model (Hindmarsh and Rose 1984) and benefit from the Nelson's stochastic mechanics (Nelson 1966 and 1967), in the dissipation existence, to model the ion channel noise impacts on the membrane voltage dynamics. The topological noise impact on the neuron dynamics gets to be more important in membranes that are small in size. Accordingly, the

DSM neuron functions like the Hindmarsh-Rose model when the membrane size is too large.

The motion equations for both variables cumulate are resulted from the formalism of the DSM neuron. The second cumulates that depict the neuron's diffusive manners do not concern us in this thesis. The first cumulates develop in harmony with the dynamics below:

$$m\dot{X} = \Pi + S_5 I$$

$$\dot{\Pi} = -\left(\frac{3a}{m}X^2 - \frac{2b}{m}X + S_0\right)(\Pi + S_5 I) - S_1 a X^3 + S_2 X^2 + S_6 X - S_6 X_{eq}(I) + S_1 I$$
$$+ S_7 - (1-r)k\left(1 - \frac{\varepsilon_m^y}{m}\right)z + (1-k)\left(1 - \frac{\varepsilon_m^z}{m}\right)y$$

$$\dot{y} = -y - dX^2 + c + \eta^y$$

$$\dot{z} = -rz + rh(X - x_s) + \eta^z$$

$$\Pi(t_0) = \mathrm{y}(t_0) - \mathrm{z}(t_0) - \mathrm{a}\big(X(t_0)\big)^3 + b\big(X(t_0)\big)^2 + (1 - S_5)I(t_0)$$

Here X indicates the membrane voltage value expected, and Π matches to the expected value of a momentum-like operator. The additional variables y and z describe the fast and the slower ion dynamics, respectively. I stands for the exterior current inserted into the neuron, and m represents the capacitance of the membrane. The variables a, b, c, d, r, and h are constants. k is a mixing coefficient presented by $k = 1/(1+r)$. S_i are constants as shown next:

$$S_0 := k + (1-k)r$$

$$S_1 := S_0 - \left[k\frac{\varepsilon_m^y}{m} + (1-k)r\frac{\varepsilon_m^z}{m}\right]$$

$$S_2 := k\left(1 - \frac{\varepsilon_m^y}{m}\right)(b-d) + (1-k)\left(1 - \frac{\varepsilon_m^z}{m}\right)(rb-d)$$

$$S_3 := k\varepsilon_u^y + (1-k)\varepsilon_u^z$$

$$S_4 := k\frac{\varepsilon_m^y}{m}(1-k)\frac{\varepsilon_m^z}{m}$$

$$S_5 := 1 - S_4$$

$$S_6 := S_3 - S_5 rh$$

$$S_7 := (rhx_s + c)S_5$$

Equation $\Pi(t_0)$ specifies the value of at the initial time in terms of the initial values of the other dynamical variables *X*, *y* and *z*, and the current *I*. $X_{eq}(I)$ obeys the equation

$$aX_{eq}^3 - (b-d)X_{eq}^2 + h\left(X_{eq} - X_s\right) - c - I = 0$$

Here X_s is a constant, η^y and η^z in equations ($\dot{y}$) and ($\dot{z}$) are Gaussian white noises with zero means and mean squares given by

$$< \eta^y(t)\eta^y(t') >= 2mT\delta(t-t')$$

and

$$< \eta^z(t)\eta^z(t') >= 2rmT\delta(t-t')$$

Were obtained by means of the classical fluctuation-dissipation theorem. T here is a temperature-like parameter. The terms with the correction coefficients ε_m^y, ε_u^y, ε_m^z and ε_u^z that take place in the above equations are the renormalization terms. Then the colored formulation for the conductances describes the autocorrelation time of $\psi_K - [\psi_K]$ is not zero and the algebraic sign of it is durable (at a microscopic timescale), ψ_K read as

$$\psi_K = [\psi_K] + Q_K$$

Here Q_K is a stochastic variable with zero expectation value at equilibrium and has some autocorrelation time greater than zero. Hence, the variable Q_K can be treated as colored noise. For the analytical implementation of NCCP, it suffices to elaborate Q_K. Then the colored formulation developed above for the potassium conductances can similarly be developed for the sodium conductances. But $\psi_{Na} - [\psi_{Na}]$ also has a finite but nonzero autocorrelation time

$$\psi_K = n^4 + \sigma_K q_K$$

$$\psi_{Na} = m^3 h + \sigma_{Na} q_{Na}$$

Chapter 4

THE MEMBRANE DYNAMICS

The sHH models incorporate some noise terms (white or colored) into the deterministic HH equations as follows:

$$CV = -g_K(n^4 + \emptyset_K)(V - E_K) - g_{Na}(\dot{m}^3 h + \emptyset_{Na})(V - E_{Na}) - g_L(V - E_L) + I$$

$$\dot{n} = \alpha_n(1 - n) - \beta_n n + \eta_n$$

$$\dot{m} = \alpha_m(1 - m) - \beta_m m + \eta_m$$

$$\dot{h} = \alpha_h(1 - h) - \beta_h h + \eta_h$$

4.1 The Fox and Lu model

In Fox & Lu model (1994), the noise terms -$\emptyset_K$and $\emptyset_{Na}$– are equal to zero:

$$\emptyset_K^F = \emptyset_{Na}^F = 0 \qquad (23)$$

While the letter F is used to denote the type of the model, and the terms $n_n, n_m, and n_h$ with the mean squares are Gaussian white noise.

$$\langle \eta_n(t)\eta_n(t')\rangle^F = \frac{\alpha_n(1-n)+\beta_n n}{N_K}\delta(t - t') \qquad (24)$$

$$\langle \eta_m(t)\eta_m(t')\rangle^F = \frac{\alpha_m(1-m)+\beta_m m}{N_{Na}}\delta(t - t') \qquad (25)$$

$$\langle \eta(t)\eta_h(t')\rangle^F = \frac{\alpha_h(1-h)+\beta_h h}{N_{Na}}\delta(t - t') \qquad (26)$$

Here $N_K$and N_{Na}denote the channel's number of potassium and sodium in the membrane.

4.2 The Linaro et al. Model

In their model Linaro (2011) use the suitable variables powers of deterministic gating in determining the proportions of open channels. Nevertheless, some processes of Ornstein-Uhlenbeck, with the diffusions acquired from the co-variances of $n^4 and m^3 h,$ escort the conductances. In consequence, the noise term escorting potassium conductance $\emptyset_K^L$, is as follow:

$$\emptyset_K^L = \sum_{i=1}^{4} Z_{K,i} \qquad (27)$$

Here $Z_{K,i}$ are stochastic variables conforming:

$$\tau_{K,i}\dot{Z}_{K,i} = -Z_{K,i} + \alpha_{K,i}\sqrt{2\tau_{K,i}\xi_{K,i}} \qquad (30)$$

Here the coefficients $\tau_{K,i}$and $\alpha_{K,i}$ are some functions of the closing and opening rates of n-gates (available in Linaro et al., 2011), and the $\xi_{K,i}$are independent unitary variances and Gaussian white noise with zero means. The noise term related with sodium channels$\emptyset_K^L$is as follow:

$$\emptyset_{Na}^L = \sum_{i=1}^{4} Z_{Na,i} \qquad (31)$$

Here $Z_{Na,i}$ are stochastic variables which obey:

$$\tau_{Na,i}\dot{Z}_{Na,i} = -Z_{Na,i} + \alpha_{Na,i}\sqrt{2\tau_{Na,i}\xi_{Na,i}} \qquad (32)$$

Here the coefficients $\tau_{Na,i}$and $\alpha_{Na,i}$are some functions of the closing and opening rates of m-gates and h-gates (available in Linaro et al., 2011), and the $\xi_{Na,i}$ are independent unitary variances and Gaussian white noise with zero means. The noise terms for the gating variables in the differential equations are paced to be zero:

$$\eta_n^L = \eta_m^L = \eta_h^L = 0 \qquad (33)$$

Thus, the degree in the gating variables of stochasticity is not predicted by the Linaro et al. (2011) formulation.

4.3 The Güler Model

None of the noise terms are placed to be zero in Güler's model (2013b). The noise terms escorting the conductances $\emptyset_{Na}^G$and $\emptyset_K^G$were inserted to capture NCCP. Both terms $\emptyset_{Na}^G$and $\emptyset_K^G$ are functions of the gating variables: the previous is dependent on $n, m, and\ h$. The term$\emptyset_K^G$, which reflects NCCP attributed to the potassium channels, is given by:

$$\emptyset_K^L = \sqrt{\frac{n^4(1-n^4)}{N_K} q_K} \qquad (34)$$

Here q_K variable obeys the differential equation of stochastic,

$$\tau \dot{p}_k = p_K \qquad (35)$$

$$\tau \dot{p}_k = -\gamma_K p_K - \varpi_K^2[\alpha_n(1-n) + \beta_n n]q_K + \xi_K \qquad (36)$$

Here ξ_K with the mean square is mean zero Gaussian white noise term,

$$\langle \xi_K(t)\xi_K(t')\rangle = \gamma_K T_K[\alpha_n(1-n) + \beta_n n]\delta(t-t') \qquad (37)$$

In equations 35 and 36 the parameter τ denotes the unit time. The constants are in dimensionless units with the following values:

$$\gamma_K = 10$$

$$\varpi_K^2 = 150$$

$$T_K = 400$$

The term $\emptyset_{Na}^G$, which reflects NCCP attributed to the potassium channels, is given by:

$$\emptyset_{Na}^L = \sqrt{\frac{n^4(1-n^4)}{N_{Na}} q_{Na}} \qquad (38)$$

Here q_{Na} variable obeys the differential equation of stochastic,

$$\tau \dot{q}_{Na} = p_{Na} \qquad (39)$$

$$\tau \dot{p}_{Na} = \gamma_{Na} p_{Na} - \varpi_{Na}^2 [\alpha_n(1-n) + \beta_n n] q_{Na} + \xi_{Na} \qquad (40)$$

Here ξ_{Na} with the mean square is mean zero Gaussian white noise term,

$$\langle \xi_{Na}(t) \xi_{Na}(t') \rangle = \gamma_{Na} T_{Na} [\alpha_n(1-n) + \beta_n n] \delta(t-t') \qquad (41)$$

The constants are in dimensionless units with the following values:

$$\gamma_{Na} = 10, \varpi_{Na}^2 = 200, T_{Na} = 800$$

The noise terms related with the variables gating are Gaussian and the mean squares satisfy:

$$\langle \eta_n(t) \eta_n(t') \rangle^G = \frac{\alpha_n(1-n) + \beta_n n}{4N_K} \delta(t-t') \qquad (42)$$

$$\langle \eta_m(t)\eta_m(t')\rangle^G = \frac{\alpha_m(1-m)+\beta_m m}{3N_{Na}}\delta(t-t') \qquad (43)$$

$$\langle \eta_h(t)\eta_h(t')\rangle^G = \frac{\alpha_h(1-h)+\beta_h h}{N_h}\delta(t-t') \qquad (44)$$

The n_h variance is the same as in the Fox and Lu model (1994), but the variances of $n_n$and n_m are one-fourth and one-third of the conforming Fox and Lu variances, respectively.

These variances are from the non-equilibrium statistical mechanics, and the stochastic variables $\mathrm{q_K}$ and $\mathrm{q_{Na}}$crop the following variances, respectively, at equilibrium:

$$\langle q_K^2\rangle_{eq} = \frac{T_K}{2\varpi_K^2} \qquad (45)$$

And

$$\langle q_{Na}^2\rangle_{eq} = \frac{T_{Na}}{2\varpi_{Na}^2} \qquad (461)$$

Table 1: Constants of membrane

C	Membrane capacitance	1 $\mu F/\mathrm{cm}^2$
g_K	Maximal potassium conductance	36 $\mathrm{mS/cm}^2$
E_K	Potassium reversal potential	-12 mV
g_{Na}	Maximal sodium conductance	120 $\mathrm{mS/cm}^2$
E_{Na}	Sodium reversal potential	115 mV
g_L	Leakage conductance	0.3 $\mathrm{mS/cm}^2$
E_L	Leakage reversal potential	10.6 mV
	Density of potassium channels	18 chns/$\mu\mathrm{m}^2$
	Density of sodium channels	60 chns/$\mu\mathrm{m}^2$

We note here that equations 45 and 46 were given above (Güler, 2013a) without dividing the coefficient 2. That was a simple typing error with no effect on result or any subsequent formulation in it.

In this model it is important to check the numerical implementation after each step of time, whether the noise terms in equations 8 to 10 takes $n_n, n_m,$ or n_h outside of the range [0, 1]. Then the step should be repeated with new random numbers for $n_n, n_m,$ or n_h.

4.4 The Functions of Noisy Rate

A typical set of noisy rate functions used by the Hodgkin-Huxley equations is as follows:

$$\alpha_n = (0.1 - 0.01V)/(exp(1 - 0.1V) - 1) \quad (47.a)$$

$$\beta_n = 0.125exp(-V/80)) \quad (47.b)$$

$$\alpha_m = (2.5 - 0.1V)/(exp(2.5 - 0.1V) - 1) \quad (47.c)$$

$$\beta_m = 4exp(-V/18) \quad (47.d)$$

$$\alpha_h = 0.07exp(-V/20) \quad (47.e)$$

$$\beta_h = 1/(exp(3 - 0.1V) + 1) \quad (47.f)$$

The constant membrane parameters values are usually used along with the rate functions mentioned in Table 1.

Due to the objective of having noisy rate functions, we modified the above standard functions as follows:

$$\alpha_n \leftarrow \alpha_n(1 + \kappa \sin(5V^n)) \quad (48.a)$$

$$\beta_n \leftarrow \beta_n(1 - \kappa \sin(5V^n)) \quad (48.b)$$

$$\alpha_m \leftarrow \alpha_m(1 - \kappa \sin(5V^m)) \quad (48.c)$$

$$\beta_m \leftarrow \beta_m(1 - \kappa \sin(5V^m)) \quad (48.d)$$

$$\alpha_h \leftarrow \alpha_h(1 - \kappa \sin(5V^h)) \quad (48.e)$$

$$\beta_h \leftarrow \beta_n(1 - \kappa \sin(5V^h)) \quad (48.f)$$

Here $V^n, V^m,$ andV^h are Ornestein-Uhlenbeck processes identified by:

$$\dot{V}^n = 50V^n + R^n \quad (49.a)$$

$$\dot{V}^m = 50V^m + R^m \quad (49.b)$$

$$\dot{V}^h = 50V^h + R^h \quad (49.c)$$

Here $R^n, R^m,$ andR^h are independent mean zero Gaussian white noise, with the mean square:

$$\langle R^n(t)R^n(t')\rangle = \langle R^m(t)R^m(t')\rangle = \langle R^h(t)R^h(t')\rangle = 100\delta(t - t')$$

In equations (49) and (50) the constants were set to be 50 and 100, respectively, for better convenience. The parameter κ is constant, which specifies the strength of the noisy rate, thus it must satisfy:

$$0 \leq |\kappa| \leq 1$$

The mean squared values of $V^n, V^m,$ and$V^h$from the properties of Ornestein-Uhlenbeck processes, obey:

$$\langle (V^n)^2\rangle = \langle (V^m)^2\rangle = \langle (V^h)^2\rangle = 1$$

in the long time limit.

The use of sinusoids in equation (48) sets a border on the effect of the introduced processes, which makes sure that the new rates never come to be negative. In equation (48), $\alpha_n$andβ_n were modified by using the identical noise term but with mutually opposite signs, as were $\alpha_m$andβ_n, $\alpha_h$andβ_h, because an effect that causes an increase in $\alpha_n$should simultaneously cause a decrease in β_n, and vice versa. For example, in order to see the voltage changes effect, consider the functions $\alpha_n$and$\beta_n$as given in equations (47.a) and (47.b). It can be found easily that, mutual derivation of $\alpha_n$and β_n with respect to V are always opposite signs. The property also applies to the functions $\alpha_m$and β_m, and$\alpha_h$and β_h. In presenting noise into the rate functions, the motivation was to acquire a challenging channel dynamics for the mathematical examination of viability and generality of the stochastic Hodgkin-Huxley models. Furthermore, it was argued that the noise existence in the rate functions is a sensible physiological reality for finite size of membranes.

4.5 The NCCP Essence

Considering that this study was directly motivated by NCCP, it is helpful to emphasize the essentials of this phenomenon before turning to the study focus. (Güler, 2011.)

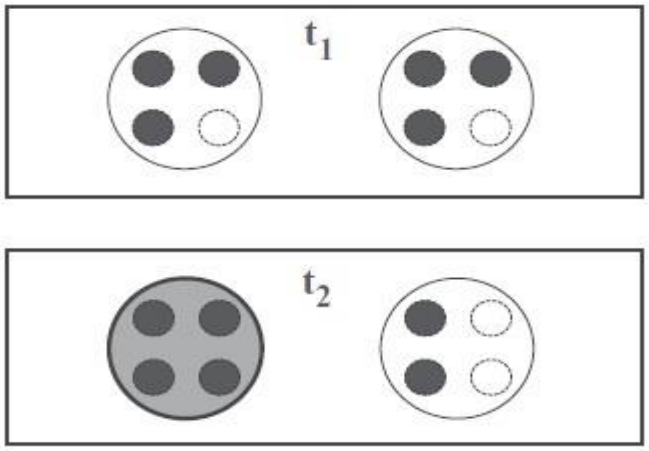

Figure 3: Two possible cases of the toy membrane. The small circles represent the gate (empty close, black open). (Güler, 2011).

Figure 3: Depiction of gate-to-channel uncertainty. Two possible conformational states of a toy membrane, comprising just two potassium channels, are shown at two different times *t*1 and *t*2. Filled black dots and small circles represent open and closed gates, respectively. The bigger circles represent channels. Despite the numbers of open gates at *t*1 and at *t*2 being the same (six), one channel (shadowed) is open at *t*2 while no channel is open at *t*1. Adopted from Güler (2011).

$\psi_K - [\psi_K]$

Due to the presence of a multiple number of n-gates in individual potassium channels, knowing n does not suffice to specify ψ_K uniquely. In paper Güler, we coined the term gate-to-channel uncertainty to describe this lack of uniqueness (see Figure 3); and the term gate noise to denote the random fluctuations in n. It was stated that the construct $\psi_K - [\psi_K]$ singles out the channel fluctuations that arise from gate-to-channel uncertainty. Here designates averaging over the possible configurations of the membrane having $4N_k n$ open n-gates. Unless the membrane is extremely small, it holds that

$$[\psi_K] \approx n^4$$

It was shown in paper Güler that a non-transient correlation takes place between the fluctuations of the construct $\psi_K - [\psi_K]$ and the fluctuations of V within the phase of subthreshold activity. This is the phenomenon that NCCP refers to. A property, crucial for the occurrence of NCCP, is that the autocorrelation time of the construct $\psi_K - [\psi_K]$ is finite but not zero. It can be deduced from sHH equation that if $\psi_K - [\psi_K] > 0$ throughout some period of time, then a negative variation, relative to the case of having $\psi_K - [\psi_K] = 0$, takes place in V along that period. Similarly, if

$\psi_K - [\psi_K] < 0$ throughout the period, then a positive variation in V takes place. Then, provided that the residence time of $\psi_K - [\psi_K]$ in the same algebraic sign is long enough, NCCP materializes. A pictorial explanation is provided in Figure 4. The construct that reveals the gate-to-channel uncertainty associated with the sodium channels is $\psi_{Na} - [\psi_{Na}]$. The configuration average of the proportion of open sodium channels, $[\psi_{Na}]$, obeys

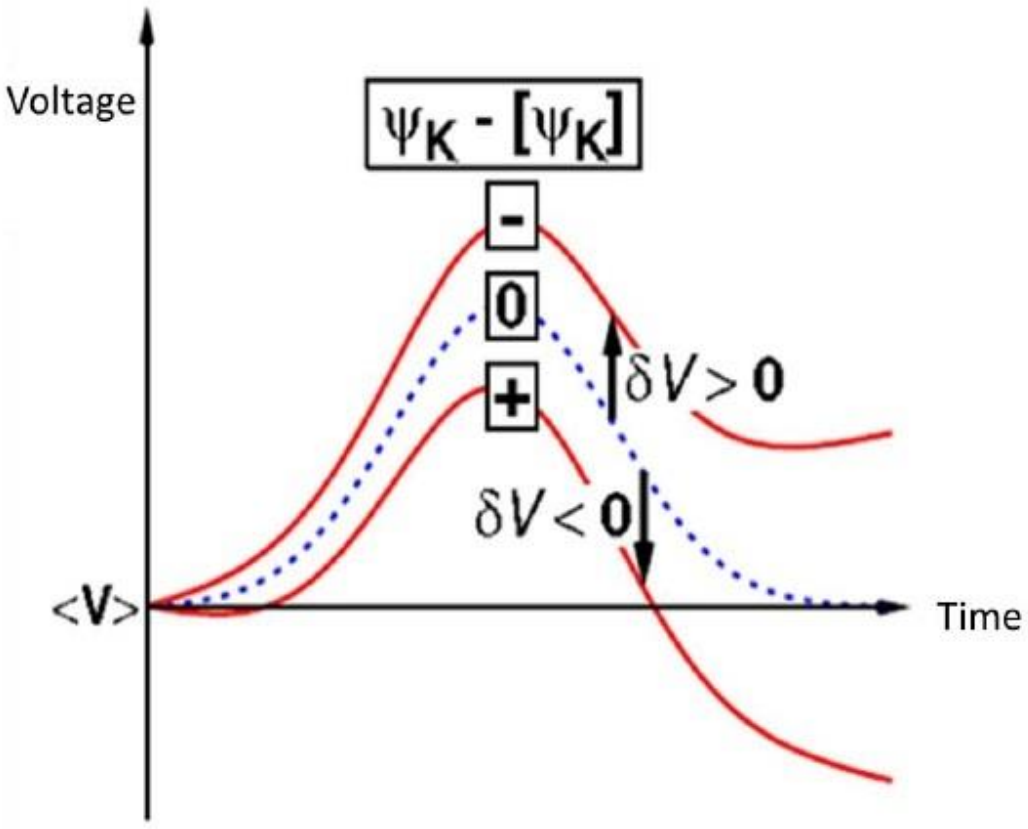

Figure 4: Explanation in the diversity of the voltage V (Güler, 2011).

Figure 4: An illustration of the variation in the voltage, denoted by δV, in response to deviations of the construct $\psi_K - [\psi_K]$ from zero. Adopted from Güler (2011).

$$[\psi_{Na}] \approx m^3 h$$

Chapter 5

NUMERICAL EXPERIMENTS

5.1 Introduction

In this part, we evaluate neuronal dynamics under the noisy rate functions articulated by equations (48) and (49) through numerical experiments. The valuation develops statistics and computations from the microscopic simulations and the Güler (2013a) colored model. As the simulation scheme of microscopic, here used the simple stochastic method (see, e.g., Zeng & Jung, 2004) by using the Markov scheme all the gates are simulate individually.

It is useful before the investigation with the new rate functions to give a representative instance on the spike generation statistics using the standard noise-free rate functions. Figure 5 provides such an example where (A) with a membrane size is 360 of potassium channels and 1200 sodium channels was used and (B) with 1800 of potassium channels with 6000 of sodium channels. The mean spiking frequencies shown in these figures, acquired from each Hodgkin-Huxley models and the microscopic scheme, as a functions of the stochastic input current. (For an overall account of the accuracy of the Linaro et al. and the Güler models, see Linaro et al., 2011; Güler, 2013; for the extent of the failure of the Fox and Lu model, see Zeng & Jung, 2004; Mino et al., 2002; Sengupta et al., 2010; ; Bruce, 2009; Güler, 2013b).

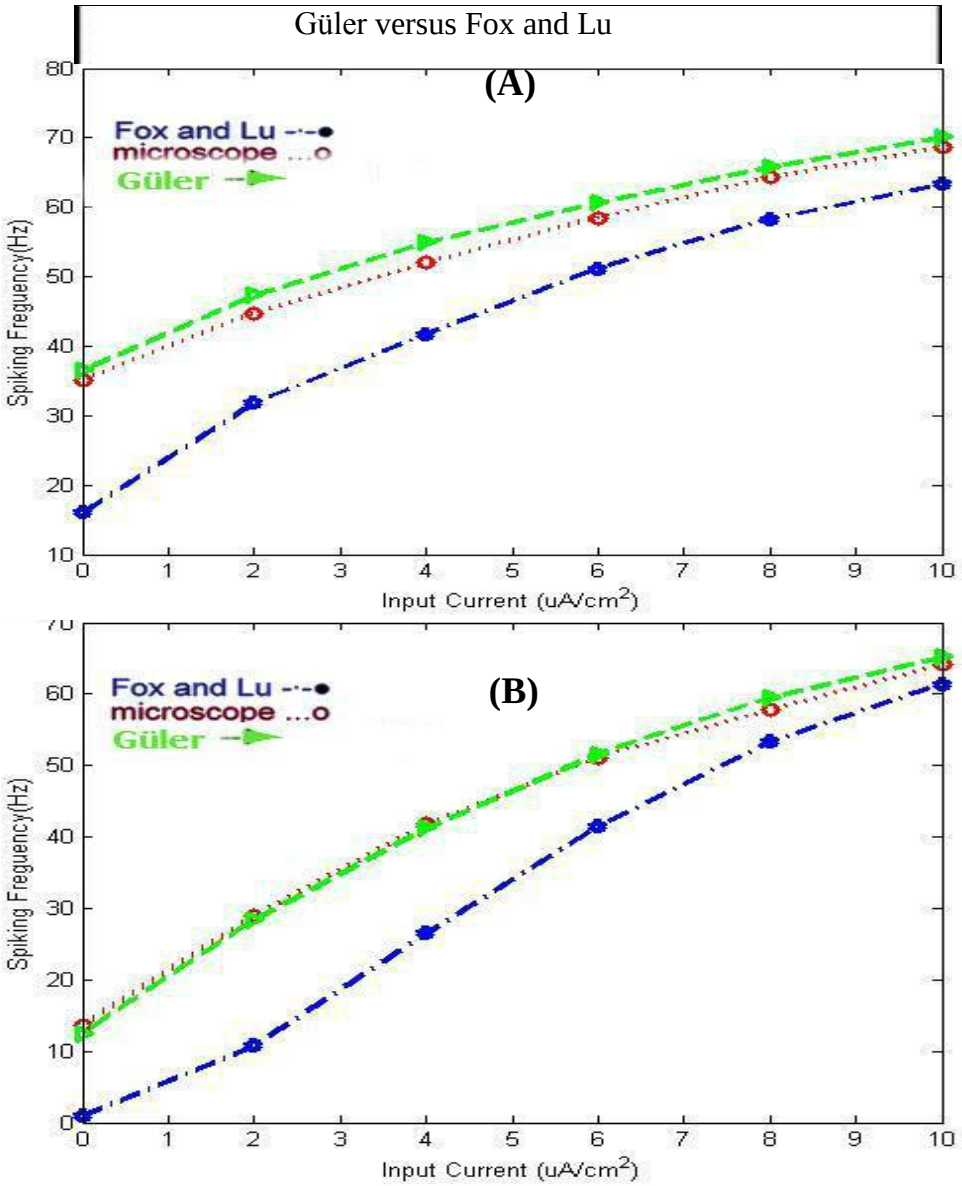

Figure 5: Result of Güler model versus Fox and Lu model

Spiking frequencies against the input current with the noise-free rate functions. Plots correspond to the microscopic simulations, the Fox and Lu model, and the Güler model. (A) 360 potassium channels and 1200 sodium channels, (B) 1800 potassium channels and 6000 sodium channels.

Figure 5 Shows the mean spiking frequency and other given information the Güler model is so closed to microscopic at the beginning of simulation but the Fox and Lu is far to the microscopic curve, the average computed over 30 sec with K=0.9.

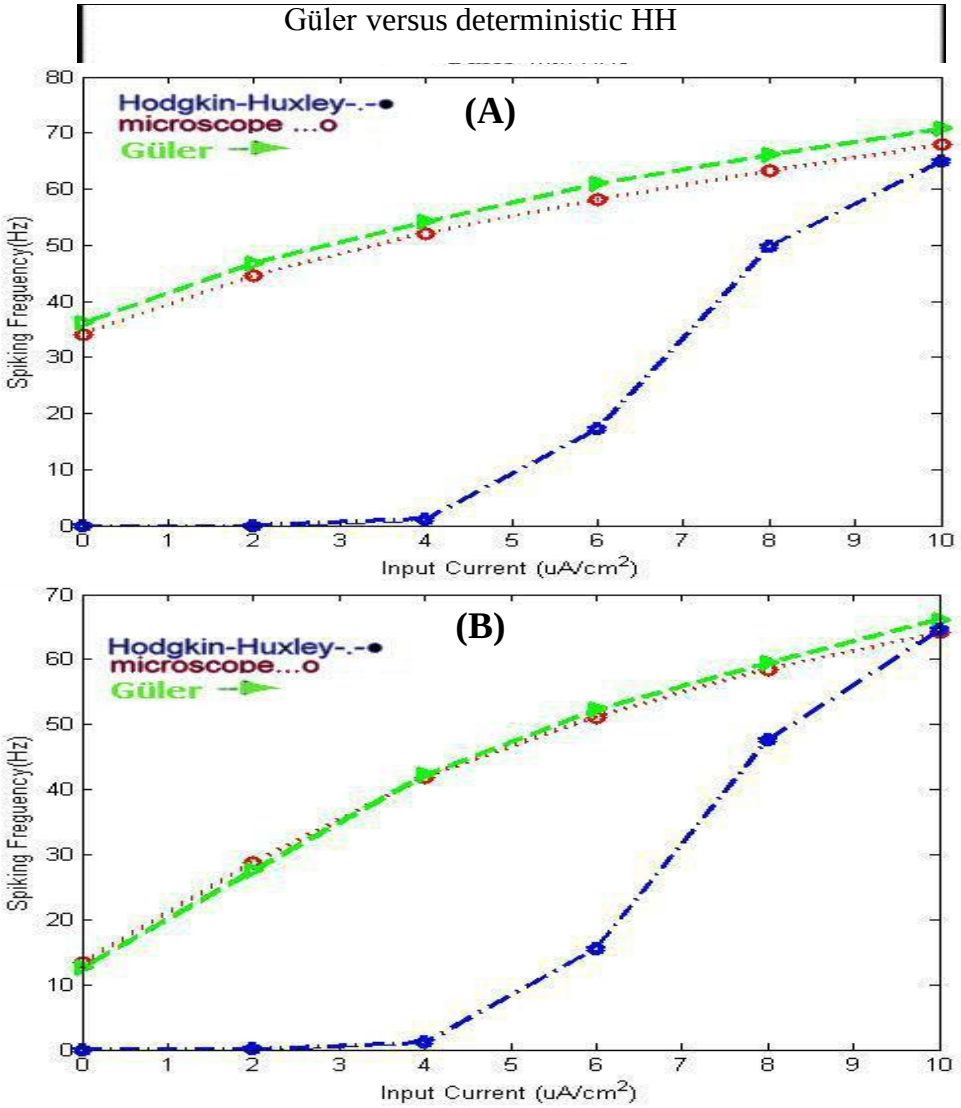

Figure 6: Result of Güler model versus deterministic Hodgkin-Huxely

Figure 6 shows spiking frequencies against the input current with the noise-free rate functions. Plots correspond to the microscopic simulations, the deterministic HH model, and the Güler model. (A) 360 potassium channels and 1200 sodium channels, (B) 1800 potassium channels and 6000 sodium channels. shows the Güler model closed to the microscope curve at the beginning of the simulation, but the deterministic HH curve is so far to the microscope curve till plot 4 and increased to close to the microscope curve till the end of the simulation that's computed over 30 sec with K=0.9.

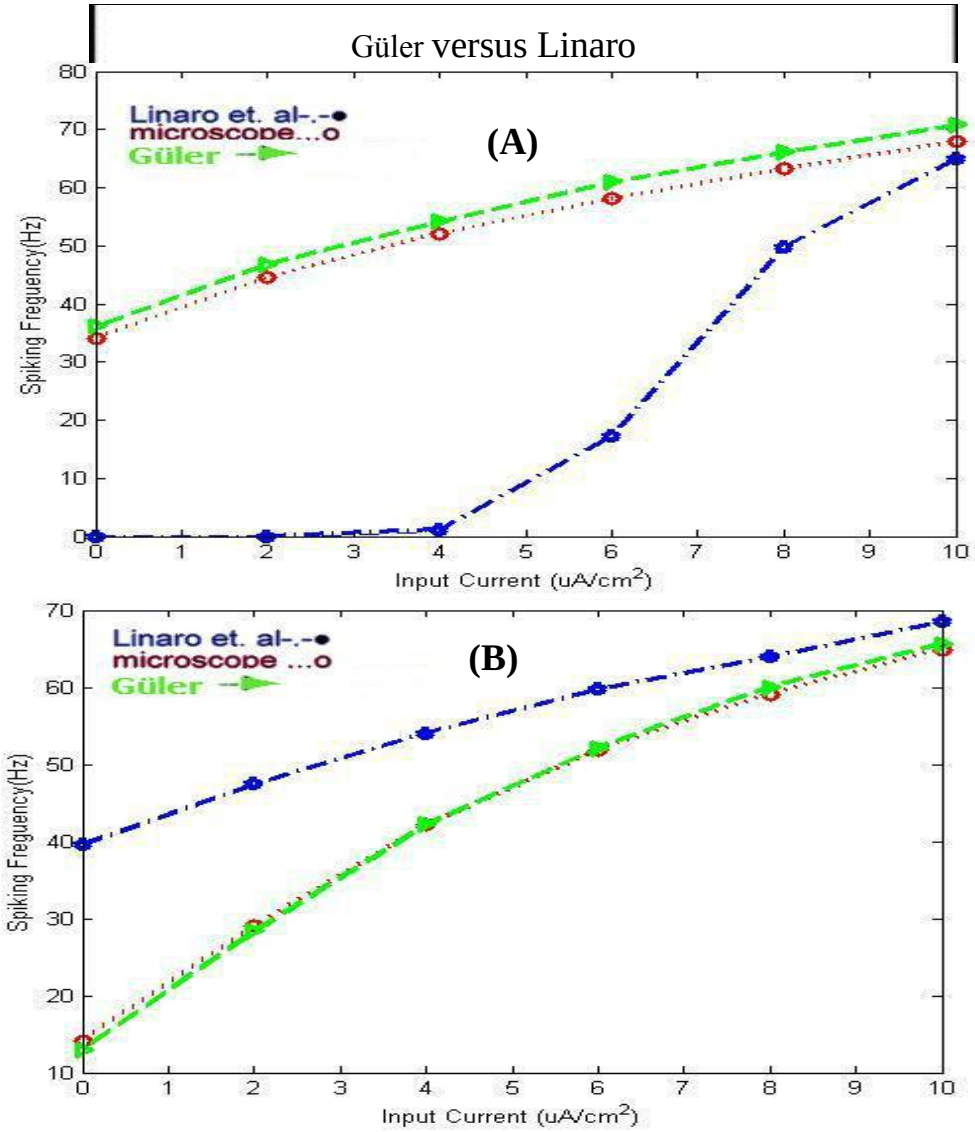

Figure 7: Result of Güler model versus Linaro et al model

Figure 7 shows spiking frequencies against the input current with the noise-free rate functions. Plots correspond to the microscopic simulations, the Linaro et al model, and the Güler model. (A) 360 potassium channels and 1200 sodium channels, (B) 1800 potassium channels and 6000 sodium channels. And the Güler model closed to the microscope curve at the beginning of the simulation, but the Linaro curve is far to the microscope curve with increasing to close to the microscope curve till the end of the simulation that's computed over 30 sec. with K=0.9.

5.2 Response to a Stimulus Pulse

After that, we studied the response of model to passing stimulus change. Using a stimulus pulse shown in Figure 8 and a sub-threshold current value, $I = -4_{\mu}A/cm^2$, was used as the base current. For a $1\ ms$ of duration, the current swerves from the foundation, arriving some value generated by intensity. We have computed latency, firing efficiency, and jitter for a set of intensities. Presenting the results are in Figures 9 to 13. Each plot in the figures was included by reiterated trials of the corresponding stimulus pulse 2000 times. Here, efficiency of firing is the part of trials that raises a spike, latency is the spike incidence mean value with regard to the stimulation over the time, and jitter of the firing latency is the standard deviation. Our equations from the figures are clears that's induce replies in a very good convention with the properties of the replies induce by the simulations of microscopic, whereas differ considerably with the results from Fox and Lu equations. Such difference between the Fox and Lu equations and microscopic simulations was reported before by other researchers (Zeng & Jung, 2004; Mino et al.,2002; Linaro et al., 2011; Bruce, 2009 ;).

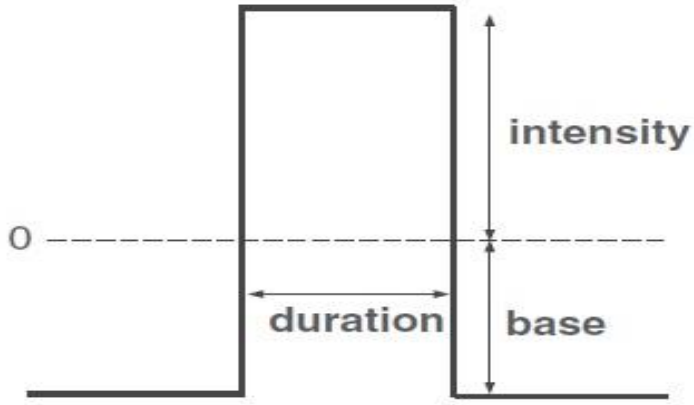

Figure 8: Form of wave of the stimulus pulse

This form in figure (8) used in section 5.5 there were used many different values of the pulse intensity in this experiments. The input current was set to $I = -4_{\mu}A/cm^2$, in 1 ms duration.

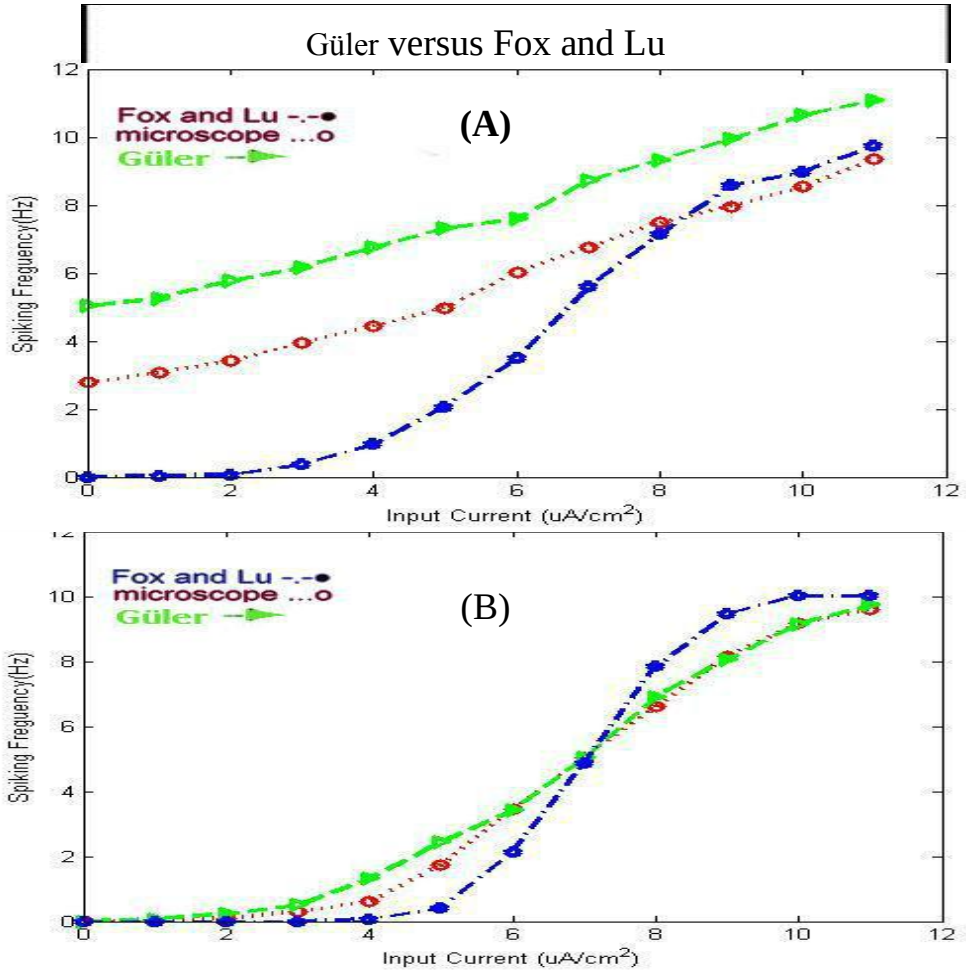

Figure 9: Result of Güler model versus Fox and Lu ($I = -4_{\mu}A/cm^2$)

The mean spiking frequency and other given information in figure 9 (A) shows the solution till the plot 6 the Güler model is closed to microscopic at the beginning of simulation and the Fox and Lu curve far to the microscopic curve and after plot 6 the Fox and Lu curve start increasing to close to microscope curve and without changing after reaching plot 10.03 that's make Güler model closer and better than Fox and Lu model, but in figure 9 (B) the Güler model closed to microscope at the beginning of simulation, the average computed over 30 sec with K=0.9.

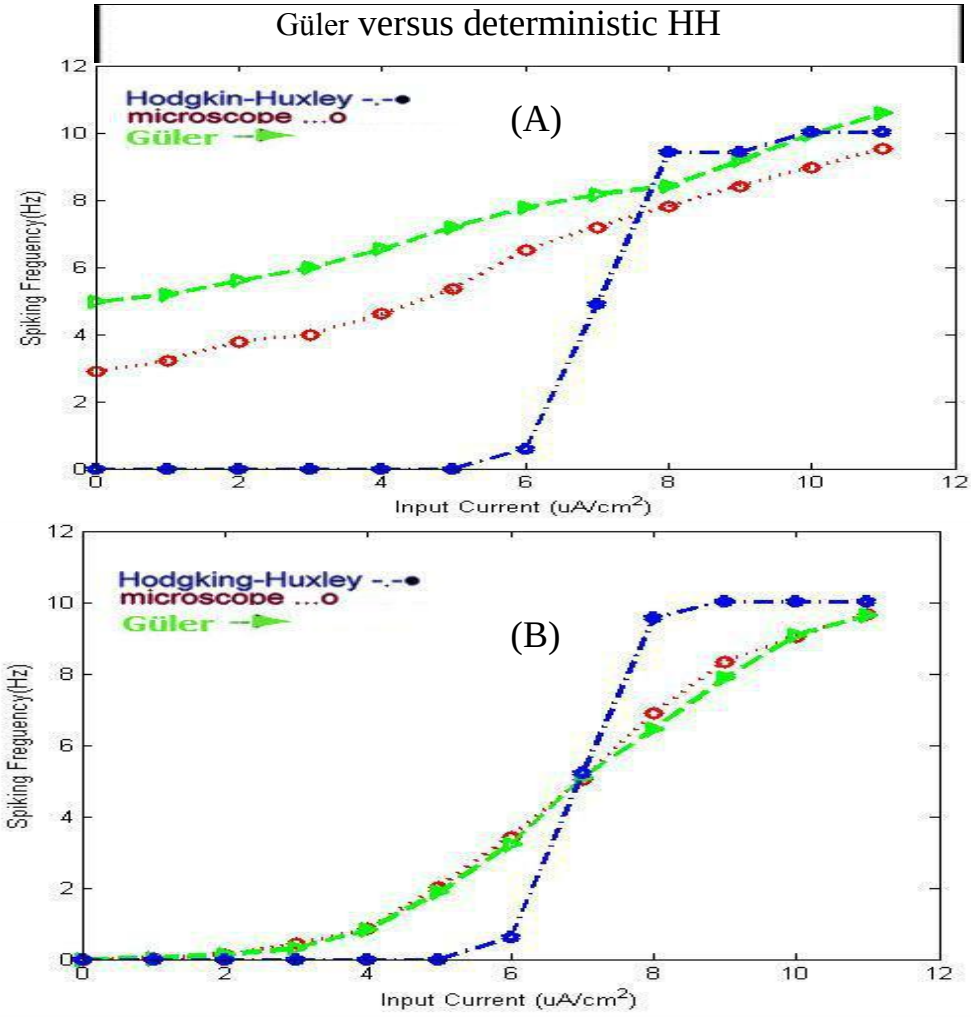

Figure 10: Result of Güler model versus deterministic Hodgkin-Huxley ($I = -4_{\mu}A/cm^2$)

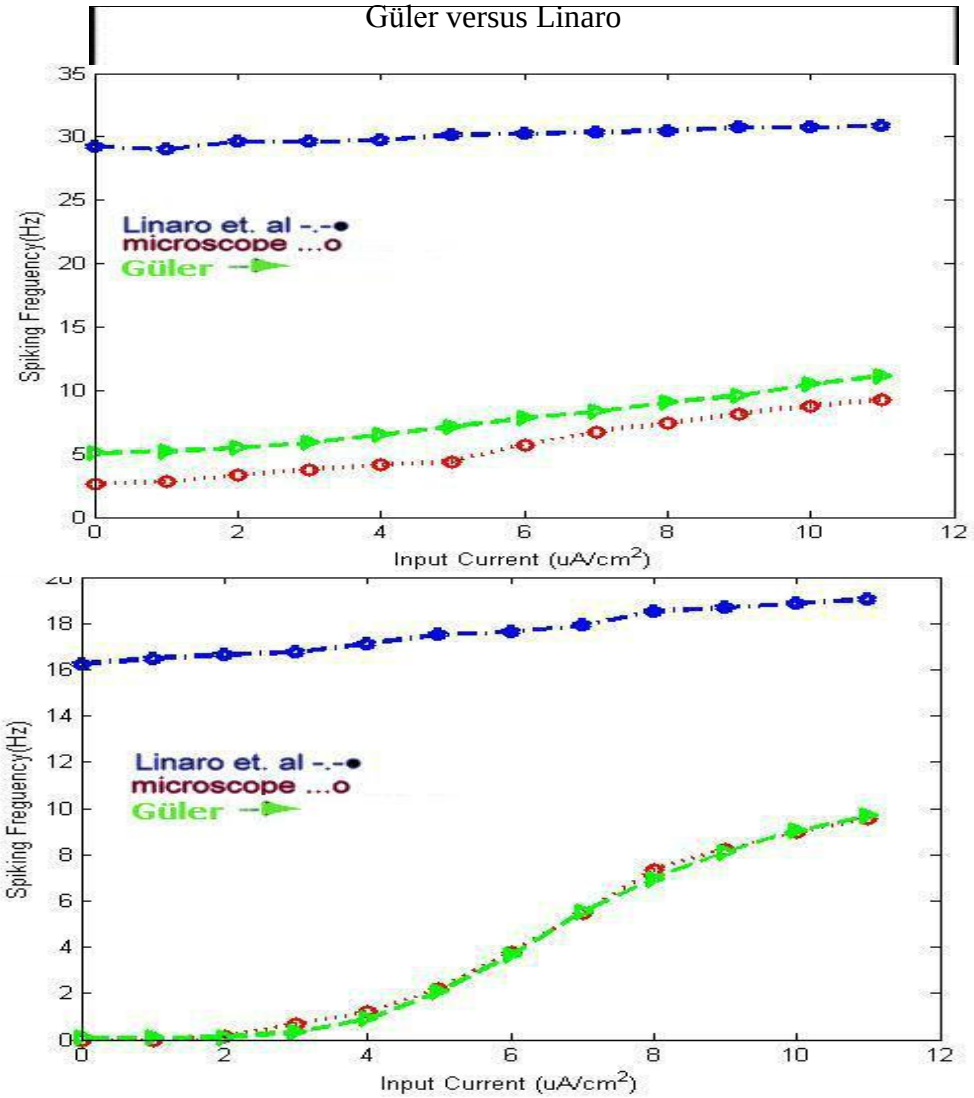

Figure 11: Result of Güler model versus Linaro et al $(I = -4_{\mu}A/cm^2)$

In figures (10) and (11) has the same result that's the Güler model is closer one to microscopic simulation. And also in figures (12) and (13) has the same result with noise-strength [0.3,0.7].

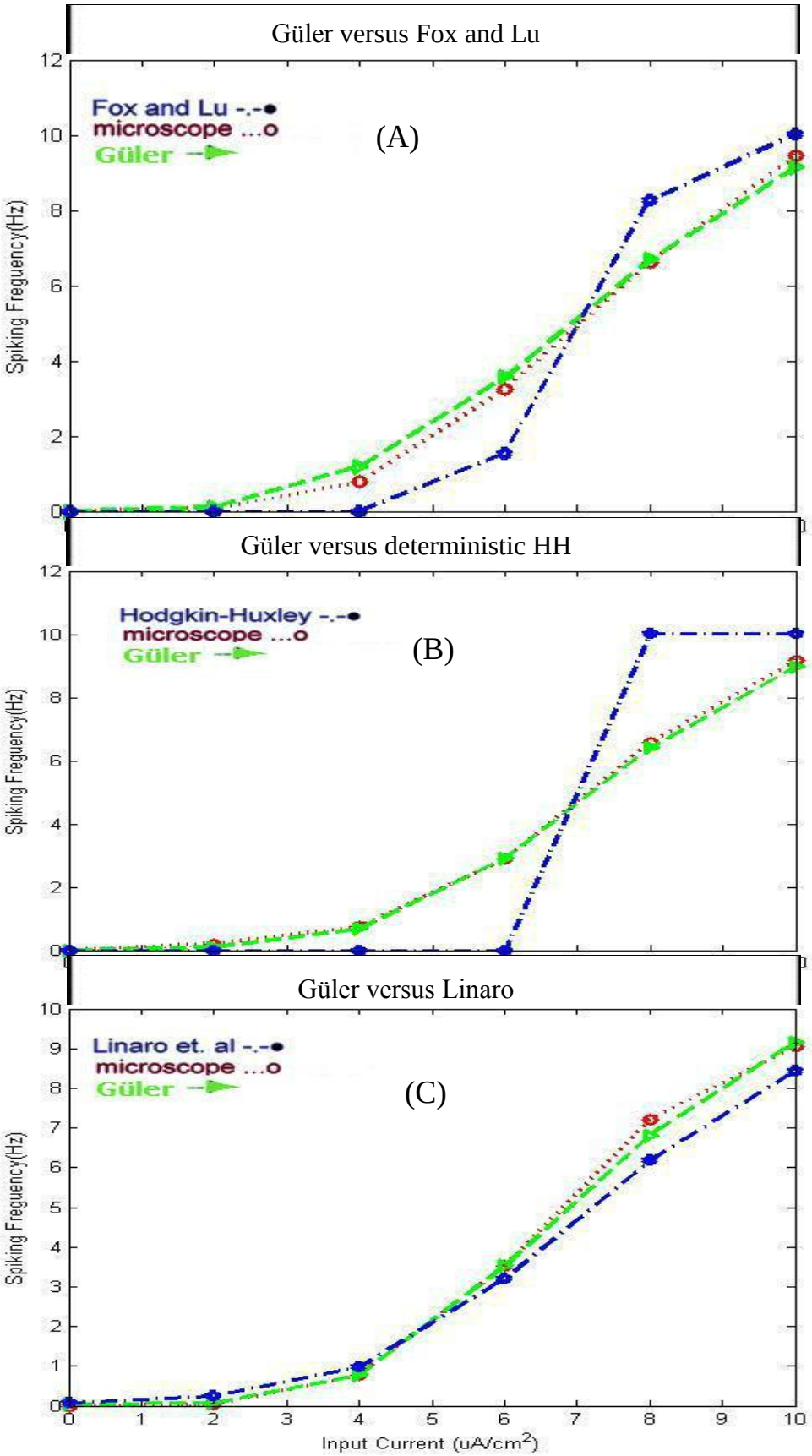

Figure 12: Results with noise strength k=0.3

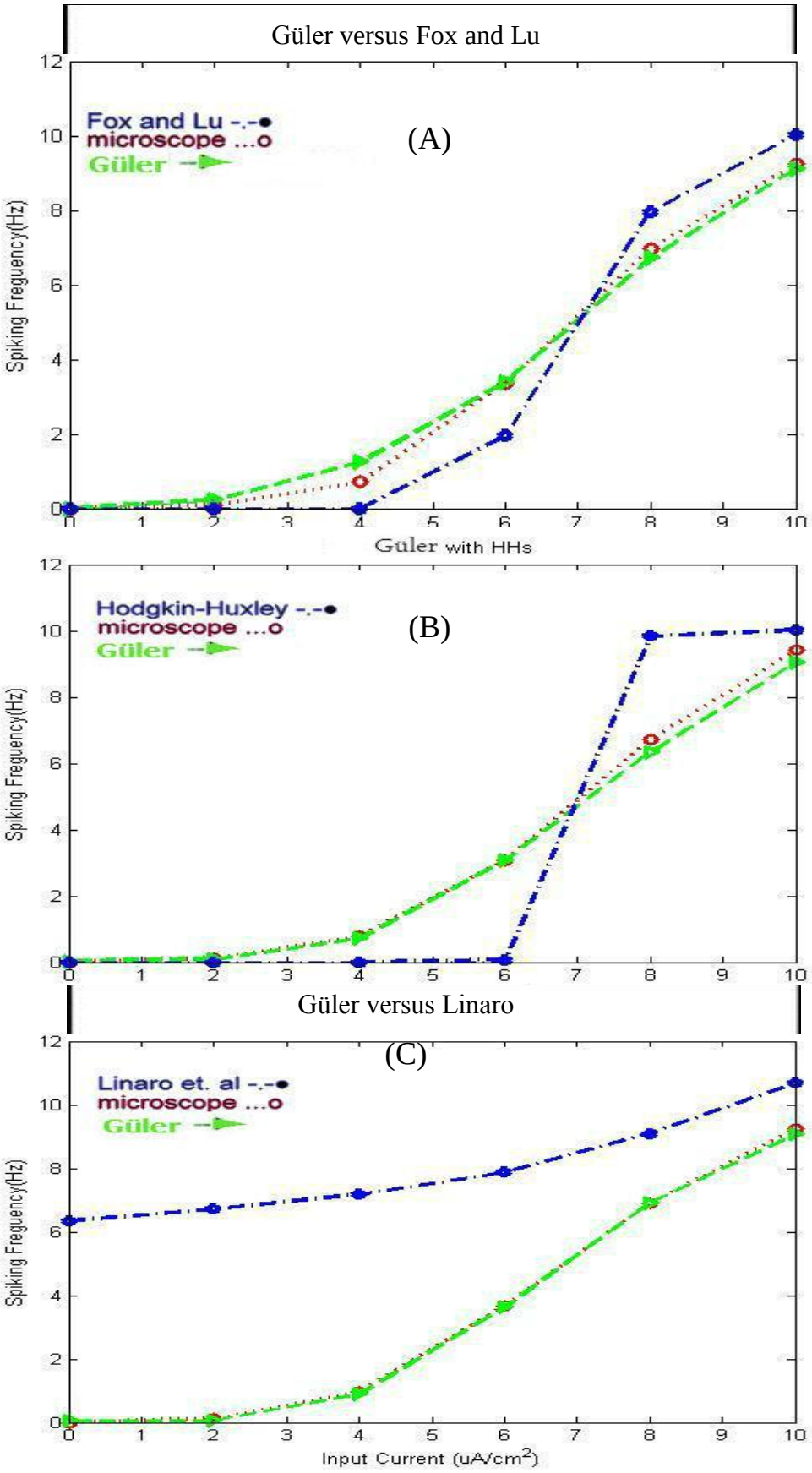

Figure 13: Results with noise strength k=0.7

Chapter 6

CONCLUSION

In this study, we have presented noise of the rate functions and are continuing experiments to examine the way in the form sHH model perform under that type of spiking statistical of noise has been studied under effects of different input signals. In an latest work (Güler, 2011), in the ion channel was found a multiplicity of the gates and the key role which will arouse the NCCP is shortcut of (non – trivially cross correlation persistent) and previously found to be the primary reason for the increase of the rise in the excitability of cells and in the spontaneous firing in small size of membrane. Also the NCCP process in promoting they found a spontaneous firing even when the size of the membrane with all of big size the is inefficient to activate the cell to the noise. This study shows that the optimization of the coherence spike is caused by the presence of the NCCP.

Our experiments show that the noise rate function is the deal with the phenomenon of the NCCP accuracy and can also be seen that the rate of spiking is caused by a model of very close to the Güler model with noise strength k=0.9, with any size of the membrane. When the width was changed model the spiking is not affected by different of sHH model, Linaro et al. and Fox and Lu model, which are far from the point of actual neuron numbers like in figures (5, 6, and 7) in each case of performing models simulation. When used varying frequency the spikes caused by noise rate functions, is also the Güler model close to the microscope, but in the

Linaro et al. model the frequencies increased but also still Güler model closer to the microscope as figure 7 the situation has remained stable at this condition .

Next, we studied the response of model to passing change in the stimulus using a stimulus pulse shown in figures (9, 10, and 11) with a sub-threshold current value, $I = -4_{\mu}A/cm^2$, used as the base current. For a $1\ ms$ of duration shown in figure 8. We have computed latency, jitter, firing efficiency for a set of intensities. Presenting the results are in Figures 9 to 11. Each plot in figures was included via reiterated trials of the corresponding pulse stimulus 2000 times. In this studying shown in figures (9, 10, and 11) the Güler model still closer one to the microscope with a low frequencies in case of performing Fox and Lu, and sHH models, and increasing frequency in case of performing Linaro et al. model with steady state of closer model (Güler model) to microscope simulation, even in different noise strength when we changed to K=0.3 and K=0.7 as shown in figures 12 and 13 which still Güler model the closer one to the microscopic curve.

It should be noted here that the width changes with the variation of different frequency to see what noise rate function to handle the amount of noise that is another option. It is also possible to use the frequencies used in the experiment with different noise and see which simulation would reply. Last but not least, the use of different frequencies, which is identical to the frequency used in experiments or different sizes are also worth investigating.

REFERENCES

Abbot, D. P. (2002). Theoretical Neuroscience Computation and Mathematical Modeling of Neural System. MIT press.

Bezrukov, S. &. (1995). Noise-induced enhancement of signal transduction across voltage-dependent ion channels. Nature, 378, 362–364.

Chow, C. C. (1996). Spontaneous action potentials due to channel fluctuations. Biophysical Journal, 71, 3013–3021.

DeFelice, L. J. (1992). Chaotic states in a random world: Relationship between the nonlinear differential equations of excitability and the stochastic properties of ion channels. Journal of Statistical Physics, 70, 339–354.

Diba, K. L. (2004). Intrinsic noise in cultured hippocampal neurons: Experiment and modeling. Journal of Neuroscience, 24, 9723–9733.

Dorval, A. D. (2005). Channel noise is essential for perithreshold oscillations in entorhinal stellate neurons. Journal of Neuroscience, 25, 10025–10028.

Faisal, A. A. (2007). Stochastic simulations on the reliability of action potential propagation in thin axons. PLoS Computational Biology, 3, 79.

Faisal, A. S. (2008). Noise in the nervous system. nervous system. Nature Reviews Neuroscience, 9, 292–303.

Güler, M. (2007). Dissipative stochastic mechanics for capturing neuronal dynamics under the influence of ion channel noise: Formalism using a special membrane. Physical Review E, 76,041918.

Güler, M. (2008). Detailed numerical investigation of the dissipative stochastic mechanics based neuron model. Journal of Computational Neuroscience, 25, 211–227.

Güler, M. (2011). Persistent membranous cross correlations due to the multiplicity of gates in ion channels. Journal of Computational Neuroscience ,31,713-724.

Güler, M. (2013a). Stochastic Hodgkin-huxley equations with colored noise terms in the conductances. Neural Computation .25:46-74, 2013.

Güler, M. (2013b). An Investigation of the Stochastic Hodgkin-Huxley Models Under Noisy Rate Functions. Neural Computation.25:2355–2372, 2013.

Hille, B. (2001). Ionic channels of excitable membranes (3rd ed.). Massachusetts: Sinauer Associates.

Hodgkin, A. L. (1952). A quantitative description of membrane current and its application to conduction and excitationin in nerve. Journal of Physiology. (London.Print), 117, 500–544.

Izhikevich, E. M. (2007). Dynamical Systems in Neuroscience:The Geometry of Excitability and Bursting. MIT press.

Jacobson, G. A. (2005). Subthreshold voltage noise of rat neocortical pyramidal neurons. Journal of Physiology, 564,145–160.

Johansson, S. &. (1994). Single-channel currents trigger action potentials in small cultured hippocampal neurons. Proceedings of National Academy of Sciences USA, 91, 1761–1765.

Jung, P. &. (2001). Optimal sizes of ion channel clusters. Europhysics Letters, 56, 29–35.

Koch, C. (1999). Biophysics of computation: Information processing in single neurons. Oxford University Press.

Kole, M. H. (2006). Single Ih channels in pyramidal neuron dendrites: Properties, distribution, and impact on action potential output. Journal of Neuroscience, 26, 1677–1687.

Lynch, J. &. (1989). Action potentials initiated by single channels opening in a small neuron (rat olfactory receptor). Biophysical Journal, 55, 755–768.

Ochab-Marcinek, A. S. (2009). Noise-assisted spike propagation in myelinated neurons. Physical Review E, 79, 011904(7).

Özer, M. (2006). Frequency-dependent information coding in neurons with stochastic ion channels for subthreshold periodic forcing. Physics Letters A, 354, 258–263.

Rowat, P. F. (2004). State-dependent effects of Na channel noise on neuronal burst generation. Journal of Computational Neuroscience, 16, 87–112.

Rubinstein, J. (1995). Threshold fluctuations in an N sodium channel model of the node of Ranvier. Biophysical Journal,68, 779–785.

Sakmann, B. &. (1995). Single-channel recording (2nded.). New York: Plenum.

Schmid, G. G. (2001). Stochastic resonance as a collective property of ion channel assemblies. Europhysics Letters, 56, 22–28.

Schneidman, E. F. (1998). Ion channel stochasticity may be critical in determining the reliability and precision of spike timing. Neural Computation, 10, 1679–1703.

Segev I., J. M. (2003). Cable and compartment models of dendritic trees in bower. The book of genesis 5:55, 2003.

Sigworth, F. J. (1980). The variance of sodium current fluctuations at the node of Ranvier. Journal of Physiology. (London Print), 307, 97–129.

Strassberg, A. F. (1993). Limitations of the Hodgkin–Huxley formalism: Effects of single channel kinetics on transmembrane voltage dynamics. Neural Computation 5, 843–855.

Whishaw, K. B. (2012). Fundamentals of Human Physiology FOURTH EDITION. Virginia United States.

White, J. A. (1998). Noise from voltage-gated ion channels may influence neuronal dynamics in the entorhinal cortex. Journal of Neurohysiology, 80, 262–269.

Zeng, S. &. (2004). Mechanism for neuronal spike generation by small and large ion channel clusters. Physical Review E, 70, 011903(8).